VORTEX CREEP AGAINST TOROIDAL FLUX LINES, CRUSTAL ENTRAINMENT, AND PULSAR GLITCHES

Erbil Gügercinoğlu[1] and M. Ali Alpar[2]
[1] Faculty of Science, Department of Astronomy and Space Sciences, Istanbul University, Beyazıt, 34119 Istanbul, Turkey; egugercinoglu@gmail.com
[2] Faculty of Engineering and Natural Sciences, Sabancı University, Orhanlı, 34956 Istanbul, Turkey; alpar@sabanciuniv.edu
Received 2014 April 17; accepted 2014 May 12; published 2014 May 23

ABSTRACT

A region of toroidally oriented quantized flux lines must exist in the proton superconductor in the core of the neutron star. This region will be a site of vortex pinning and creep. Entrainment of the neutron superfluid with the crustal lattice leads to a requirement of superfluid moment of inertia associated with vortex creep in excess of the available crustal moment of inertia. This will bring about constraints on the equation of state. The toroidal flux region provides the moment of inertia necessary to complement the crust superfluid with postglitch relaxation behavior fitting the observations.

Key words: dense matter – pulsars: general – stars: magnetic field – stars: neutron

1. INTRODUCTION

Glitches are sudden increases in rotation rates of pulsars, with $\Delta\Omega/\Omega \sim 10^{-9}$–$10^{-6}$, usually accompanied by jumps in the spin-down rate, $\Delta\dot{\Omega}/\dot{\Omega} \sim 10^{-4}$–$10^{-2}$ (Espinoza et al. 2011; Yu et al. 2013). These changes tend to relax fully or partially on long timescales (days to years), attributed to superfluid components of the neutron star (Baym et al. 1969). The electromagnetic signals of pulsars do not change at glitches, indicating that there is no change in the external torque, so that glitches reflect angular momentum exchange between the observed crust and interior components of the neutron star (see Weltevrede et al. 2011 for a notable exception). The energy source of large glitches is rotational kinetic energy, which is the minimal free energy source available for the large and frequent exchanges of angular momentum. If additional free energy sources like elastic or magnetic energy were involved, the accompanying energy dissipation would exceed the observational bounds on glitch associated thermal radiation (Alpar 1998). Starquake models can account for the smaller glitches typified by the Crab pulsar. Starquakes also act as triggers for the large glitches (Alpar et al. 1996). A superfluid with quantized vortices which can be pinned will explain the exchange of angular momentum discontinuously as seen in the glitches (Packard 1972; Anderson & Itoh 1975), if large numbers of vortices unpin in an avalanche which can be self-organized (Melatos et al. 2008), or triggered by a starquake.

The vortex pinning and creep model (Alpar et al. 1984a) explains glitches and postglitch response in terms of moments of inertia and relaxation times of the neutron superfluid in the neutron star crust's crystal lattice, where vortex lines can pin to nuclei. Pinning leads to a lag $\omega = \Omega_s - \Omega_c > 0$ between superfluid and crustal angular velocities Ω_s and Ω_c. As vortex lines pin and unpin continually by thermal activation, the lag ω drives an average vortex current radially outward from the rotation axis. This "vortex creep" allows the superfluid to spin down. The system evolves toward a steady state at which superfluid and the crust spin down at the same rate, $\dot{\Omega}_s = \dot{\Omega}_c = \dot{\Omega}_\infty$, achieved at the steady state lag ω_∞. In addition to the continual spin-down by vortex creep, if ω reaches a critical value ω_{cr} beyond which pinning forces can no longer sustain the lag, a sudden discharge of the pinned vortices occurs. The resulting angular momentum transfer to the crust is observed as a glitch. The superfluid rotation rate decreases by

$\delta\Omega_s$ and the crust rotation rate increases by $\Delta\Omega_c$, so that the lag decreases by $\delta\omega = \delta\Omega_s + \Delta\Omega_c$ at the glitch. This glitch-induced change in ω offsets the creep, leading to very slow relaxation of the spin-down rate by the creep as thermal activation has a nonlinear dependence on ω. There is also a linear regime of creep leading to prompt exponential relaxation from some parts of the superfluid.

The superfluid core of the star is already coupled to the crust tightly (Alpar et al. 1984b; Easson 1979), on timescales short compared to the glitch rise time, which is less than 40 s for the Vela pulsar (Dodson et al. 2002). When the interaction between vortex lines and flux lines is included the crust–core coupling timescale becomes even shorter (Sidery & Alpar 2009). The core superfluid is thus effectively included in the observed spin-down of the outer (normal matter) crust and magnetosphere. The effective crust moment of inertia I_c includes the core superfluid, so that $I_c \cong I$, the total moment of inertia of the star. The jump and relaxation in the observed spin-down rate of the crust indicates that the moment of inertia fraction in crustal superfluid participating in the glitch and postglitch relaxation is $\Delta\dot{\Omega}_c/\dot{\Omega}_c \sim I_{cr-sf}/I$. The observed $\Delta\dot{\Omega}_c/\dot{\Omega}_c \sim 10^{-3}$–$10^{-2}$ is consistent with the crustal superfluid moment of inertia fraction for neutron stars. This was proposed as a potential constraint for the equation of state (Datta & Alpar 1993; Lattimer & Prakash 2007, and references therein).

Superfluid neutrons in the inner crust are in Bloch states of the crust lattice. Their effective mass m_n^* is larger than the bare neutron mass m_n (Chamel 2005, 2012). This "entrainment" leaves only a fraction of the neutron superfluid to be effectively free to store and exchange angular momentum with the lattice (Chamel & Carter 2006; Andersson et al. 2012; Chamel 2013). The fractional change in the observed spin-down rate must be multiplied by the enhancement factor $m_n^*/m_n > 1$. The total moment of inertia in pinned superfluid sustaining vortex creep, I_{creep}, must be large enough, such that $I_{creep}/I \sim (m_n^*/m_n)\Delta\dot{\Omega}/\dot{\Omega}$. The required moment of inertia in components of the star with pinning/creep then exceeds the moment of inertia of the crustal superfluid, $I_{creep} > I_{cr-sf}$, for reasonable neutron star equations of state (Andersson et al. 2012; Chamel 2013). This suggests the involvement of the core superfluid in glitches and postglitch relaxation.

In the core, protons are expected to form a type II superconductor with a dense array of flux lines (Baym et al. 1969). If present at all, type I superconductivity exists near the star's

center, at $\rho > 2\rho_0$ (Jones 2006). Vortices can pin to flux lines by minimization of condensation and magnetic energies when vortex and flux line cores overlap (Sauls 1989; Ruderman et al. 1998). Arguments for type I superconductivity based on putative precession (Link 2003) are invalidated by the possibility of vortex creep (see Alpar 2005 and references therein). The work of Haskell et al. (2013) based on Vela glitches, concluding for either weak flux–vortex pinning or type I superconductivity, also does not take creep into account. Type II superconductivity with flux–vortex pinning and creep will accommodate the observed glitch and postglitch behavior.

The bulk of the core proton superconductor–neutron superfluid region is likely to carry a uniform or poloidal array of flux lines. The associated moment of inertia fraction is too large, beyond the requirement of the entrainment effect. Furthermore, a uniform or poloidal arrangement of the flux lines offers easy directions for vortex line motion without pinning or creep. This will make the effect of pinning and creep in the core dependent on the angle between the rotation and magnetic axes, making the moment of inertia fractions involved highly variable among different pulsars. A toroidal arrangement of flux lines, by contrast, provides a topologically unavoidable site for pinning and creep, and can have conditions similar to those of pinning against nuclei in the crustal lattice (Sidery & Alpar 2009). We discuss toroidal arrangement of flux lines in neutron stars as a site of vortex pinning and creep and its implications for pulsar glitches.

2. THE TOROIDAL MAGNETIC FLUX IN NEUTRON STARS

In normal (non-superconducting) stars, like the progenitors of neutron stars, purely toroidal (Tayler 1973) or poloidal (Wright 1973) magnetic fields are unstable. Spruit (1999) has found that for stability of magnetic fields in stratified stars, the toroidal B_ϕ to poloidal B_p field ratio satisfies

$$\frac{B_\phi^2}{B_p} < \frac{Nr^2\rho^{1/2}}{l_h}, \tag{1}$$

where ρ is density, l_h is the horizontal length scale of the perturbations which can be as large as the stellar radius R, and r is the cylindrical radial coordinate. N, the buoyancy frequency of the stratified medium, has a typical value of 500 s^{-1} in neutron stars (Reisenegger & Goldreich 1992). For a very young neutron star which has not yet cooled below the superconducting-superfluid transition temperatures, we obtain $B_\phi \lesssim 10^{14}$ G by taking $l_h \sim r \sim R \sim 10^6$ cm, $\rho \sim 10^{14}$ g cm^{-3} and $B_p \sim 10^{12}$ G. Braithwaite (2009) has shown that stable equilibrium configurations in upper main sequence stars (neutron star progenitors) have strong toroidal fields surrounding the poloidal field. A qualitatively similar field configuration is likely to be maintained as the neutron star core cools down and the core protons make the transition into the type II superconductor phase. In a neutron star with a superconducting core, a purely poloidal magnetic field in hydromagnetic equilibrium at the crust–core boundary, though not stable, is found to have a field strength of 10^{14} G corresponding to a surface magnetic field of $B_p \sim 3 \times 10^{12}$ G, typical for radio pulsars (Henriksson & Wasserman 2013). Simulations of upper main sequence stars (Braithwaite 2009) and neutron stars with superconducting cores (Lander et al. 2012; Lander 2014) have common features. The toroidal field component is confined within closed field lines of the poloidal field. The poloidal field strength is maximum at
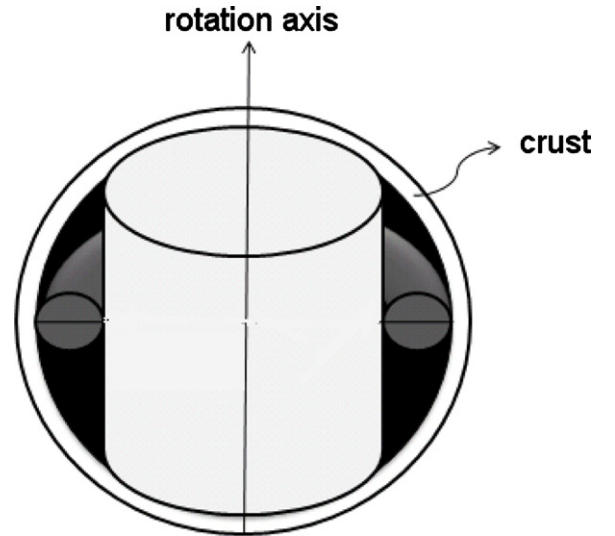

Figure 1. Sketch showing the toroidal field (gray). The black shading marks the superfluid region, with moment of inertia $I_{\rm tor}$, caused by vortices creeping against the toroidal flux. For simplicity the magnetic and rotation axes are taken to be aligned.

the stellar center, while the toroidal field attains its largest value in the outer regions, at $r > 0.5\,R$. The toroidal field is confined within the neutron star crust for poloidal fields $\lesssim 5 \times 10^{13}$ G (Lander 2014), but electron differential rotation in the crust will wind the poloidal field to generate strong toroidal flux (Gourgouliatos & Cumming 2014), which is not likely to remain confined to the crust, and will extend into the core. For a stable configuration, the ratio of the toroidal and total magnetic field energies, $E_{\rm tor}/E_{\rm mag}$ cannot be less than about 10% (Braithwaite 2009). In a model with a superconducting core and proton fluid crust, this energy ratio is found to be as large as 90% when crustal toroidal fields are included (Ciolfi & Rezzolla 2013). Thus, simulations indicate a strong toroidal magnetic field of 10^{14} G (Lander 2014; Ciolfi & Rezzolla 2013), which will be carried by the flux lines. The toroidal field is maximum at $r \sim 0.8\,R$, confined within an equatorial belt of radial extension $\sim 0.1\,R$ (Lander et al. 2012; Lander 2014). Plausible neutron star models with relatively hard equations of state have radii $R \cong 12$ km, insensitive to the mass in the $M \sim (1\text{–}2)\,M_\odot$ range. The density in the outer core is approximately uniform, $\rho \sim \rho_0 = 2.8 \times 10^{14}$ g cm^{-3}. The moment of inertia fraction controlled by vortex lines passing through the toroid, as shown in Figure 1 is estimated to be $I_{\rm tor}/I \approx 5 \times 10^{-2}$. Depending on the radial extent of the toroidal field, the moment of inertia of the associated region can be comparable to and even larger than that of the inner crust superfluid.

3. POSTGLITCH RELAXATION ACCORDING TO THE VORTEX CREEP MODEL

The observed spin-down rate $\dot{\Omega}_c$ typically displays several distinct postglitch relaxation terms with different moments of inertia and relaxation modes, including exponentially decaying transients and permanent changes in rotation and spin-down rates. Depending on the pinning energy E_p and the interior temperature T, vortex creep can operate in linear or nonlinear regimes (Alpar et al. 1989). In the linear regime, the steady state lag ω_∞ is much smaller than $\omega_{\rm cr}$. A linear creep region with moment of inertia I_l contributes an exponentially relaxing term

to the postglitch response (Alpar et al. 1993)

$$\Delta\dot{\Omega}_c(t) = -\frac{I_l}{I}\frac{\delta\omega}{\tau_l}e^{-t/\tau_l}, \quad (2)$$

with a relaxation time,

$$\tau_l \equiv \frac{kT}{E_p}\frac{R\omega_{\mathrm{cr}}}{4\Omega_s v_0}\exp\left(\frac{E_p}{kT}\right), \quad (3)$$

where $v_0 \approx 10^7$ cm s^{-1} is a microscopic vortex velocity. In a region where no glitch-induced vortex motion takes place, $\delta\omega = \Delta\Omega_c$. The Vela pulsar, the best studied glitching pulsar with glitches every $\sim$2–3 yr, typically exhibits three exponential transients, four transients being resolved if the glitch is observed immediately (Dodson et al. 2002). Other glitching pulsars show one or two transients (Espinoza et al. 2011; Yu et al. 2013).

In the nonlinear creep regime ω_∞ is very close to ω_{cr}. The contribution of a nonlinear creep region of moment of inertia I_{nl} to the postglitch response of the observed crust spin-down rate is (Alpar et al. 1984a)

$$\Delta\dot{\Omega}_c(t) = -\frac{I_{\mathrm{nl}}}{I}|\dot{\Omega}|\left[1 - \frac{1}{1 + (e^{t_0/\tau_{\mathrm{nl}}} - 1)e^{-t/\tau_{\mathrm{nl}}}}\right], \quad (4)$$

with the nonlinear creep relaxation time

$$\tau_{\mathrm{nl}} \equiv \frac{kT}{E_p}\frac{\omega_{\mathrm{cr}}}{|\dot{\Omega}|}. \quad (5)$$

We have omitted the subscript ∞ from $|\dot{\Omega}|$ as variations in the spin-down rate do not exceed a few percent. Vortices unpinned at a glitch move through some nonlinear creep regions. These parts of the superfluid are deeply affected by the resulting sudden decrease in the superfluid rotation rate with $\delta\omega \cong \delta\Omega_s \gg \Delta\Omega_c$. Creep temporarily stops, decoupling these regions from angular momentum exchange with the crust, so that the external torque now acts on less moment of inertia. Creep restarts after a waiting time $t_0 = \delta\omega/|\dot{\Omega}|$. When $t_0 \gg \tau_{\mathrm{nl}}$, Equation (4) reduces to a Fermi function recovery within a time interval of width $\sim \tau_{\mathrm{nl}}$ around t_0. The combined response for a distribution of waiting times $t_0(r) = \delta\omega(r)/|\dot{\Omega}|$, which depends on the number of unpinned vortices that move through each superfluid region, can be integrated using Equation (4). If the density of unpinned and repinned vortices is taken to be uniform throughout some superfluid regions of total moment of inertia I_A, representing a mean field approach, then the integrated contribution to $\Delta\dot{\Omega}_c(t)$ is characterized by a constant second derivative $\ddot{\Omega}_c$ with which $\dot{\Omega}_c(t)$ recovers its preglitch value after a waiting time t_0 corresponding to the maximum initial postglitch offset $\delta\omega$ in these unpinning–repinning regions (Alpar et al. 1984a). When initial transients are over, this slower response takes over. This behavior prevails in the interglitch timing of the Vela pulsar, and its healing signals the return to preglitch conditions, providing an estimate of the time of occurrence for the next glitch. Such constant $\ddot{\Omega}_c$ is common in older pulsars (Yu et al. 2013), and scales with the parameters of the vortex creep model (Alpar & Baykal 2006). Part of the glitch in Ω_c, associated with moment of inertia I_B, never relaxes back. This corresponds to vortex free regions B interspersed with the unpinning–repinning creep regions A. The vortex free regions B are analogous to capacitors in a circuit: they do not support continuous vortex currents and do not contribute to the spin-down, transferring

angular momentum only at glitches when the unpinned vortices pass through. The glitch magnitude is given by the angular momentum balance (Alpar et al. 1993):

$$I_c\Delta\Omega_c = (I_A/2 + I_B)\delta\Omega_s. \quad (6)$$

4. VORTEX CREEP AGAINST TOROIDAL FLUX LINES

Junctions with toroidal flux lines inevitably constrain motion of the vortex lines. Entrainment of the neutron and proton mass currents in the core endows a vortex with a magnetic field of $B_v = [(m_p - m_p^*)/m_n][\Phi_0/\pi\Lambda_*^2] \sim 10^{14}$ G, while the magnetic field in a flux line is $B_\Phi = [\Phi_0/\pi\Lambda_*^2] \sim 10^{15}$ G (Alpar et al. 1984b). The pinning energy due to magnetic interaction between a vortex and a flux line is of the order of $E_p = (B_v B_\Phi/4\pi) \times V$, where $V \cong 2\pi\Lambda_*^3$ is the overlap volume with the interaction range given by the London length $\Lambda_* = 29.5[(m_p^*/m_p)x_p^{-1}\rho_{14}^{-1}]^{1/2}$ fm (Alpar et al. 1984b). In the above expressions $\Phi_0 \equiv hc/2e$ is the flux quantum, m_p^* and m_p are the effective and bare mass of the proton, $x_p \sim 0.05$ is the proton fraction in the outer core, and ρ_{14} is the density in units of 10^{14} g cm^{-3}. Chamel & Haensel (2006) find $m_p^*/m_p \sim 0.5$–0.9, with $m_p^*/m_p \cong 0.5$ indicated by limits on crust–core coupling from the resolution of Vela glitches (Dodson et al. 2002). A rough estimate gives $E_p \sim 6$ MeV, though there is a wide range of estimates $E_p \sim 0.1$–10 MeV (Sauls 1989; Chau et al. 1992). Taking the range of the pinning force as $\sim\Lambda_*$ and the average length between junctions as the spacing between flux lines, $l_\Phi = (B_\phi/\Phi_0)^{-1/2}$, the maximum lag ω_{cr} that can be sustained by pinning forces is given by the Magnus equation $\rho\kappa R\omega_{\mathrm{cr}} = E_p/l_\Phi\Lambda_*$. The temperature at the crust–core boundary can be estimated for cooling via the modified Urca process (Yakovlev et al. 2011), or by relating the inner crust temperature to surface temperature measurements (Gudmundsson et al. 1983). Both methods give interior temperatures of 10^8–10^9 K. With these ranges of E_p and kT, vortex creep will be in the nonlinear regime. The nonlinear creep relaxation time does not have the uncertainties of the E_p estimate when divided by ω_{cr}, giving, scaling with Vela pulsar parameters,

$$\tau \simeq 60\left(\frac{|\dot{\Omega}|}{10^{-10}\,\mathrm{rad\,s^{-2}}}\right)^{-1}\left(\frac{T}{10^8\,\mathrm{K}}\right)\left(\frac{R}{10^6\,\mathrm{cm}}\right)^{-1}x_p^{1/2}$$
$$\times \left(\frac{m_p^*}{m_p}\right)^{-1/2}\left(\frac{\rho}{10^{14}\,\mathrm{gr\,cm^{-3}}}\right)^{-1/2}\left(\frac{B_\phi}{10^{14}\,\mathrm{G}}\right)^{1/2}\mathrm{days}, \quad (7)$$

with $\rho = 2\times10^{14}$ g cm^{-3} and $x_p = 0.05$ we obtain $\tau \cong 30$ days. The toroidal flux line region has no obvious structures to provide vortex traps. The crust lattice with its domains and dislocations, can provide vortex trap regions A and vortex free regions B interspersed with them, and is the locus of crust breaking to trigger vortex unpinning. Thus it is likely that vortices are unpinned from traps in the crust superfluid. As these vortices move outward, they do not traverse the toroidal flux region which lies further in. There is therefore no change in the superfluid rotation rate in the toroidal flux region. The offset time here is determined by the glitch in the observed rotation rate of the crust:

$$t_0 = \frac{\Delta\Omega_c}{|\dot{\Omega}|} = 7\left(\frac{t_{\mathrm{sd}}}{10^4\,\mathrm{yr}}\right)\left(\frac{\Delta\Omega_c/\Omega_c}{10^{-6}}\right)\mathrm{days}, \quad (8)$$

where $t_{sd} = \Omega/2|\dot{\Omega}|$ is pulsar spin-down age. Expanding Equation (4) in $t_0/\tau < 1$, we obtain

$$\Delta\dot{\Omega}_c(t) = -|\dot{\Omega}|\frac{I_{tor}}{I}\frac{t_0}{\tau}e^{-t/\tau}. \qquad (9)$$

We omit the mass entrainment correction $m_p^*/m_p < 1$ in the core superfluid. Its effect on estimating the moment of inertia of the superfluid controlled by the toroidal field region will be within the uncertainties in the actual extent of the toroidal region. Taking into account $m_p^*/m_p < 1$ will decrease rather than increase the value of I_{tor} to be inferred from $\Delta\dot{\Omega}_c$. This response of the nonlinear creep against toroidal flux lines is of the same form as the linear creep response of inner crust superfluid associated with postglitch exponential relaxation, Equation (2), but with the nonlinear relaxation time and offset time given by Equations (7) and (8).

5. CONCLUSIONS

The entrainment effect for the crustal superfluid requires more moment of inertia in extra-crustal superfluid regions with pinning and creep in order to account for the observed glitch related changes in the spin-down rates of pulsars. The toroidal configuration of flux lines in the outer core can provide the site for this. Creep response in this region provides an exponentially relaxing contribution to the glitch in the spin-down rate. For Vela (Alpar et al. 1993) and Crab (Alpar et al. 1996) glitches, the crustal superfluid with exponential relaxation makes up the largest part of the moment of inertia involved, $\sim 10^{-2}I$, without taking entrainment into account. There is a particular exponential relaxation component with $\tau \cong 32.7$ days in agreement with our estimate for the toroidal flux line region for the first nine Vela glitches. The amplitudes of this exponential relaxation are in the range $\Delta\dot{\Omega}_l \cong (0.58$–$1.21)10^{-2}\dot{\Omega}$ (Chau et al. 1993). The nonlinear creep response of the toroidal flux line region, as well as the linear creep response of the crustal superfluid employed in earlier work, can contribute to the observed $\Delta\dot{\Omega}_l$, as both components relax with similar relaxation times and commensurate moments of inertia. Taking into account vortex creep against toroidal flux lines, the moment of inertia fraction I_l/I in the crustal superfluid involved in exponential relaxation leads to a new constraint on the total crystalline crust moment of inertia I_{crust}:

$$\frac{I_l}{I} = \left(\frac{\Delta\dot{\Omega}_l}{\dot{\Omega}} - \frac{I_{tor}}{I}\right)\frac{m_n^*}{m_n} \sim 10^{-3}\text{–}10^{-2} < \frac{I_{crust}}{I}, \qquad (10)$$

which in principle can lead to constraints on the equation of state (Lattimer & Prakash 2007), if uncertainties in I_{tor}/I and m_n^*/m_n and the location of the crust–core boundary are resolved. With entrainment in the crustal superfluid, the angular momentum balance, Equation (6), becomes

$$\frac{\Delta\Omega_c}{\delta\Omega_s} = \frac{m_n}{m_n^*}\frac{I_A/2 + I_B}{I_c} \lesssim \frac{m_n}{m_n^*}\frac{I_{cr-sf}}{I - I_{cr-sf} - I_{tor}}. \qquad (11)$$

Using the analysis of Vela pulsar glitches with the vortex creep model (Alpar et al. 1993; Chau et al. 1993) and the estimate of $I_{cr-sf}/I \simeq 4 \times 10^{-2}$ (Lattimer & Prakash 2007), we obtain $m_n^*/m_n \lesssim 2.2$–4. This range accounts for a density range $\rho \gtrsim 6.4 \times 10^{13}$ g cm^{-3} in the inner crust (Chamel 2012, 2013). It should be noted that calculations of the enhancement factor

assume a bcc lattice that may not be valid (Kobyakov & Pethick 2013); uncertainties about defects and impurities as well as "pasta" structures may also lead to smaller enhancement factors (Chamel 2013). Recent work explores if plausible neutron star equations of state allow for a thicker crust to accommodate large enhancement factors (Steiner et al. 2014; Piekarewicz et al. 2014).

The magnetar 1RXS J170849.0−4000910 (Kaspi & Gavriil 2003) and the radio pulsar PSR B2334+61 (Yuan et al. 2010) underwent glitches with exponential relaxation for both of which $\Delta\dot{\Omega}_c/\dot{\Omega}_c \sim 0.1$, indicating moments of inertia larger than the crustal superfluid even without entrainment. The response of the toroidal field region can account for these as well. In regions without glitch associated vortex motion the response would still be exponential relaxation, and the toroidal flux line region would contribute a similar response, providing the extra moment of inertia. In older pulsars, the linear creep regions of the crustal superfluid progressively become nonlinear creep regions, and relaxation times calculated by Equation (7) become longer. In this case glitches would be step like increases with no significant relaxation. Such behavior is indeed observed (Espinoza et al. 2011; Yu et al. 2013). The exponential relaxation time τ in Equation (7), if identified from pulsars of different ages as corresponding to the toroidal flux region, can yield information on microphysical parameters and the location of the crust–core boundary.

We have given a proof of principle about the role of vortex pinning and creep response from the toroidal flux region in the outer core of the neutron star. The superfluid controlled by pinning and creep in this region can complement the crust superfluid to accommodate the moment of inertia requirements of entrainment. The vortex creep relaxation times are consistent with analysis of postglitch response in the Vela glitches and scaling of the model to other pulsars.

REFERENCES

Alpar, M. A. 1998, AdSpR, 21, 159
Alpar, M. A. 2005, in NATO ASIB Proc. 210: The Electromagnetic Spectrum of Neutron Stars, ed. A. Baykal et al. (Dordrecht: Springer), 33
Alpar, M. A., Anderson, P. W., Pines, D., & Shaham, J. 1984a, ApJ, 276, 325
Alpar, M. A., & Baykal, A. 2006, MNRAS, 372, 489
Alpar, M. A., Chau, H. F., Cheng, K. S., & Pines, D. 1993, ApJ, 409, 345
Alpar, M. A., Chau, H. F., Cheng, K. S., & Pines, D. 1996, ApJ, 459, 706
Alpar, M. A., Cheng, K. S., & Pines, D. 1989, ApJ, 346, 823
Alpar, M. A., Langer, S. A., & Sauls, J. A. 1984b, ApJ, 282, 533
Anderson, P. W., & Itoh, N. 1975, Natur, 256, 25
Andersson, N., Glampedakis, K., Ho, W. C. G., & Espinoza, C. M. 2012, PhRvL, 109, 241103
Baym, G., Pethick, C. J., & Pines, D. 1969, Natur, 224, 673
Braithwaite, J. 2009, MNRAS, 397, 763
Chamel, N. 2005, NuPhA, 747, 109
Chamel, N. 2012, PhRvC, 85, 035801
Chamel, N. 2013, PhRvL, 110, 011101
Chamel, N., & Carter, B. 2006, MNRAS, 368, 796
Chamel, N., & Haensel, P. 2006, PhRvC, 73, 045802
Chau, H. F., Cheng, K. S., & Ding, K. Y. 1992, ApJ, 399, 213
Chau, H. F., McCulloch, P. M., Nandkumar, R., & Pines, D. 1993, ApJL, 413, L113
Ciolfi, R., & Rezzolla, L. 2013, MNRAS, 435, L43
Datta, B., & Alpar, M. A. 1993, A&A, 275, 210
Dodson, R. G., McCulloch, P. M., & Lewis, D. R. 2002, ApJL, 564, L85

Easson, I. 1979, ApJ, 228, 257
Espinoza, C. M., Lyne, A. G., Stappers, B. W., & Kramer, M. 2011, MNRAS, 414, 1679
Gourgouliatos, K. N., & Cumming, A. 2014, MNRAS, 438, 1618
Gudmundsson, E. H., Pethick, C. J., & Epstein, R. I. 1983, ApJ, 272, 286
Haskell, B., Pizzochero, P. M., & Seveso, S. 2013, ApJL, 764, L25
Henriksson, K., & Wasserman, I. 2013, MNRAS, 431, 2986
Jones, P. B. 2006, MNRAS, 371, 1327
Kaspi, V. M., & Gavriil, F. P. 2003, ApJL, 596, L71
Kobyakov, D., & Pethick, C. J. 2013, PhRvC, 87, 055803
Lander, S. K. 2014, MNRAS, 437, 424
Lander, S. K., Andersson, N., & Glampedakis, K. 2012, MNRAS, 419, 732
Lattimer, J. M., & Prakash, M. 2007, PhR, 442, 109
Link, B. 2003, PhRvL, 90, 101101
Melatos, A., Peralta, C., & Wyithe, J. S. B. 2008, ApJ, 672, 1103
Packard, R. E. 1972, PhRvL, 28, 1080
Piekarewicz, J., Fattoyev, F. J., & Horowitz, C. J. 2014, arXiv:1404.2660
Reisenegger, A., & Goldreich, P. 1992, ApJ, 395, 240
Ruderman, M. A., Zhu, T., & Chen, K. 1998, ApJ, 492, 267
Sauls, J. A. 1989, in Timing Neutron Stars, ed. H. Ögelman & E. P. J. van den Heuvel (New York: Kluwer), 457
Sidery, T. L., & Alpar, M. A. 2009, MNRAS, 400, 1859
Spruit, H. C. 1999, A&A, 349, 189
Steiner, A. W., Gandolfi, S., Fattoyev, F. J., & Newton, W. G. 2014, arXiv:1403.7546
Tayler, R. J. 1973, MNRAS, 161, 365
Weltevrede, P., Johnston, S., & Espinoza, C. M. 2011, MNRAS, 411, 1917
Wright, G. A. E. 1973, MNRAS, 162, 339
Yakovlev, D. G., Ho, W. C. G., Shternin, P. S., Heinke, C. O., & Potekhin, A. Y. 2011, MNRAS, 411, 1977
Yu, M., Manchester, R. N., Hobbs, G., et al. 2013, MNRAS, 429, 688
Yuan, J. P., Manchester, R. N., Wang, N., et al. 2010, ApJL, 719, L111